DISCLAIMER NOTICE

THIS DOCUMENT IS BEST QUALITY PRACTICABLE. THE COPY FURNISHED TO DTIC CONTAINED A SIGNIFICANT NUMBER OF PAGES WHICH DO NOT REPRODUCE LEGIBLY.

62-435

THE ROLE OF THE EMISSION CHANNEL IN AN ION SOURCE

By

S. N. Popov

FTD-TT- 62-435/1+2+4

UNEDITED ROUGH DRAFT TRANSLATION

THE ROLE OF THE EMISSION CHANNEL IN AN ION SOURCE

By S. N. Popov

English pages: 11

Source: Zhurnal Tekhnicheskoy Fiziki, 31, No. 12, 1431-1438, 1961.

SC-1133
SOV/57-61-31-12

PREPARED BY:

TRANSLATION SERVICES BRANCH
FOREIGN TECHNOLOGY DIVISION
WP-AFB, OHIO.

FIRST LINE OF TEXT

THE ROLE OF THE EMISSION CHANNEL IN AN ION SOURCE

FIRST LINE OF TITLE

S. N. Popov

As is known, selection of the shape and dimensions of an emission channel determine, to a considerable extent, the density of the selected current, the utilization factor of the working gas, the electrical efficiency of the source, and the focusing of the ion beam. The anode of the source, containing the ion-emission channel, should assure considerable dissipation of the thermal energy which comes from secondary electrons and from the electrons that compensate for the space charge of the ion beam. Other reasons notwithstanding, the limiting current of the ion tube is essentially limited by the thermal strength of the anode of the source. To assure intense heat removal, the anodes in high-current ion tubes should be made thick, i.e., instead of the ordinary emission opening we have an emission channel whose length is several times the diameter. This latter fact changes essentially the selection of the ion current.

At relatively high selection potentials (usually greater than 20-25 kv), the ion-emission surface or the boundary of the gas-discharge plasma is located within the emission channel; however, the basic drop in pressure of the working gas (the pressure drop between the ion source and the region of the ion optic) takes place in the channel. This considerably complicates a theoretical examination of the process of ion-current selection.

STOP HERE STOP HERE

In this work we give the results of an investigation of the ion current as a FIRST LINE OF TEXT function of the selection potential and the geometry of the emission channel.

1. Limiting the Ion Current by a Space Charge

The Child-Langmuir law [1], known as the "3/2 law," defines the limiting current density between infinite flat electrodes (the plane case) with an applied potential difference V_a:

$$j = 5.45 \cdot 10^{-8} \frac{V_a^{3/2}}{d^2 \sqrt{A}}, \qquad (1)$$

FIRST LINE OF TITLE where j is the current density in amp/cm^2; V_a is the potential of the anode with respect to the cathode, in volts; d is the distance between electrodes, in centimeters; and A is the molecular weight of the ions which create the current.

In the case of a restricted cathode, i.e., when the cathode radius $R << d$, the total current I is calculated from the formula

$$I = 5.45 \cdot 10^{-8} \frac{V_a^{3/2} S}{d^2 \sqrt{A}} \alpha\left(\frac{R}{d}\right), \qquad (2)$$

where S is the emission area of the cathode, in cm^2; R is the cathode radius; α is the Levintov correction [2] which takes into account the action of the field in the case of a cathode of limited length.

We will use the name "hard cathode" when d is not a function of V_a in Eqs. (1) and (2).

When the electric field interacts with a gas-discharge plasma, the cathode is a certain boundary surface of the plasma, which moves in space as a function of the value of V_a, i.e., $d = f(V_a)$. In this case it is convenient to call the cathode elastic.

Kistemaker and Dekker [3, 4], investigating a magnetic ion source, found a dependence of the selected ion current on the applied selection potential in a form similar to $I = f(V_a^{3/2})$. On this basis the authors concluded that the selected ion current is limited by the space charge and is subject to the 3/2 law.

Gabovich and Kucherenko [5, 6], in an experiment using a device similar to

STOP HERE STOP HERE

that of Kistemaker and Dekker [3], showed that the value of the selected current
FIRST LINE OF TEXT
is not a function of the applied potential (in both works the selection potential did not exceed 10-15 kv). On this basis the authors concluded that the ion current in the given case is not limited by the space charge.

In all these works [3-4 and 5-6] the experimental function $I = f(V)$ was compared with (2) without taking α into account, while the area of the emission opening was taken as S and the distance between the anode and the selecting electrode was used as $\underline{d}$. Obviously, with an elastic cathode (in this case, the emission surface
FIRST LINE OF TITLE
of the plasma), the 3/2 law cannot be used without taking into account $\underline{d}$ and S as functions of V_a.

Figure 1 shows schematically the position of the electrodes in a system for selecting the current of an ion source. Let $\underline{d}$ be the distance from the selecting electrode to the edge of the plasma. We will consider that the plasma which passes from the emission opening into the space between the electrodes is in the form of a cone shown in Fig. 1. Such a concept is valid, since the space between the electrodes is a region of high vacuum and, consequently, the path lengths of the plasma components are much greater than the dimensions of the system. We can state approximately that the emission surface S is a circle formed by the cross section of the plasma cone with a plane passing at distance $\underline{d}$ from the selecting electrode. Then, from Fig. 1 we get

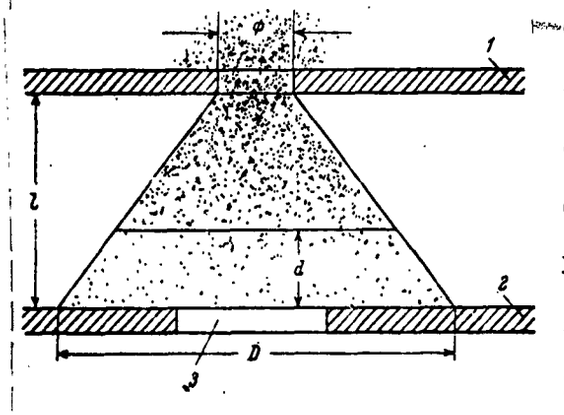

Fig. 1. Diagram of the position of the electrodes in an ion-current selection system. 1) anode of the source; 2) selecting electrode of the ion optic; 3) opening in the selecting electrode; ϕ - diameter of the emission opening; l - distance between the anode and the selecting electrode; D - diameter of the lower base of the plasma cone; $\underline{d}$ - distance from the selecting electrode to the plasma boundary.

$$\frac{d}{S^{1/2}} = \sqrt{\frac{\pi}{4}}\left[D-(D-\Phi)\frac{d}{l}\right]. \qquad (3)$$

STOP HERE

STOP HERE

Substituting (3) in (2) we get, after transformations,

$$d = \frac{3.7 \cdot 10^{-2} D \alpha^{1/2} v_a^{3/4} I^{-1/2}}{1 + 3.7 \cdot 10^{-2} (D - \Phi) e^{-1} \alpha^{1/2} v_a^{3/4} I^{-1/2}}, \qquad (4)$$

where v_a is the selection potential, in kv; I is the ion current, in amperes; d is the distance from the selecting electrode to the plasma boundary, in cm; ℓ is the distance between electrodes, in cm; Φ is the diameter of the emission opening, in cm; and D is the diameter of the lower base of the plasma cone, in cm.

Figure 2 shows d as a function of v_a, determined experimentally by Gabovich and Kucherenko [5] (curve A), and the same obtained from Formula (4) (curve B). The necessary data are taken from [5], viz., ℓ = 0.9 cm, Φ = 0.3 cm, and the value of D was determined from the ratio of the ion current passing to the receiver to the current dissipated on the selecting electrode, and was 1.6 cm. In the calculations, α was taken as unity, because of the fact that in the experiment [5] the dimension of the selecting electrode was comparable with the dimension of the plasma emission surface.

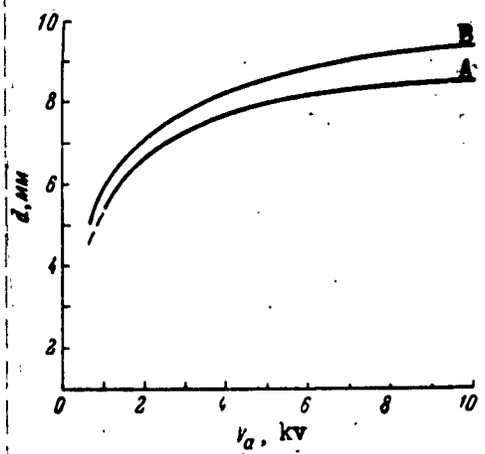

Fig. 2. Graphs of d vs. the selection potential. A - experimental curve; B - calculated curve.

The quite good agreement between the experimental and calculated curves indicates that the ion current in the examined space is limited by the space charge and is subject to the Child-Langmuir law.

2. The Boundary Region of Plasma - The External Electric Field

When plasma interacts with the wall in the near-wall region, a space-charge envelope forms [7]. The wall is negatively charged because of the electrons whose temperature in low-pressure plasma is always higher than that of the ions, while the plasma acquires a positive potential with respect to the wall.

We can show [8] that the drop in potential in the envelope is defined by the relationship

FIRST LINE OF TEXT

$$V_p = \frac{kT_e}{2e} \ln\left(\frac{m_i}{2\pi m_e}\right)^{1/4}, \qquad (5)$$

where k is the Boltzmann constant; T_e is electron temperature, in °K; e is the electron charge; and m_i, m_e are the masses of the ion and electron, respectively.

The thickness p of the envelope layer is defined by the relation

$$p = \left(\frac{kT_e}{4\pi e^2 n}\right)^{1/2} \left(\frac{1}{3} \ln \frac{m_i}{2\pi m_e}\right)^{1/4} = h\left(\frac{1}{3} \ln \frac{m_i}{2\pi m_e}\right)^{1/4}, \qquad (6)$$

where n is the concentration of ions in the plasma; and h is the Debye shielding radius.

FIRST LINE OF TITLE

From (5) and (6) we get the average potential gradient in the envelope:

$$E = \overline{\text{grad}\, V_p} = (4.5\pi n k T_e)^{1/2} \left[\ln \frac{m_i}{2\pi m_e}\right]^{1/4}. \qquad (7)$$

We can examine the interaction of plasma with an electric field in the same way as the interaction with a conducting wall at a floating potential. In our opinion, the difference is that the boundary of the external electric field must be treated as an elastic wall which moves under "pressure" of the plasma boundary field (7) until the values of the field of the plasma and the external field are equal. The indicated fields are then probably matched until a single electric field forms outside the plasma. In such a case, using the known selection current, we can determine, with the aid of (2), the distance d from a certain undisturbed equipotential of the external field to the plasma boundary.

3. The Role of the Emission Channel

Let us examine an elementary model of a magnetic arc-source for ions (Fig. 3). Let us assume that between cathode 1 and the outside of anode 2 (region I) there is such a strong magnetic field that diffusion of the ions across the magnetic field can be neglected, and further let us assume that there is no magnetic field between the outside of anode 2 and the selecting electrode 3 (region II). The anode is at ground potential, and a potential V_a is applied to the selecting electrode. For V_a close to zero the plasma penetrates into region II right up to the

STOP HERE STOP HERE

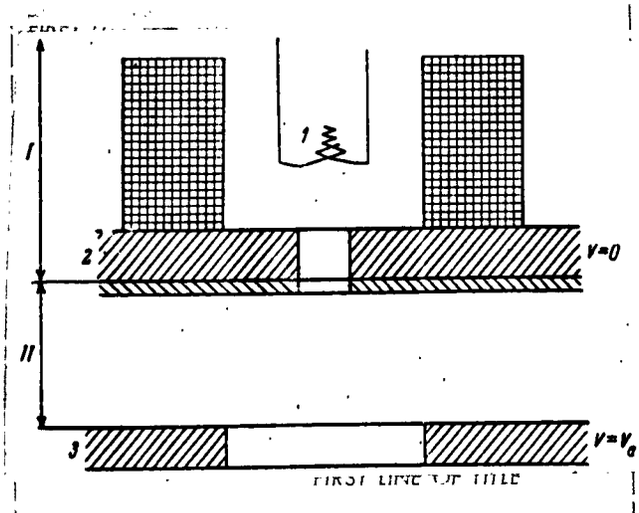

Fig. 3. Diagram of a magnetic ion source. 1 - cathode; 2 - anode; 3 - selecting electrode. I - region of strong magnetic field; II - region of very weak magnetic field.

of the working gas, the plasma is pinched and assumes cylindrical form. Now, independently of V_a, and until the boundary shifts to the other side of the channel n, T_e' and $\overline{\text{grad } V_a}$ will have a value which is approximately constant and maximum for the given arc discharge. The area of plasma-selection surface S will be preserved. Because a pinched plasma has this property, the maximum current density can be selected using a device that assures a rapid change in the external-potential gradient. The channel is just such a device.

The undisturbed potential and its gradient on the axis of the channel can be described quite accurately [9] by the formula

$$v = v_0(1 - \tanh kz), \qquad (8)$$

where v_0 is the potential on the axis at the channel axis; $k = 1.32/R$; R is the channel radius; z is the axial coordinate

$$E = |\text{grad } v| = v_0 \frac{k}{\coth^2 kz}. \qquad (9)$$

Figure 4 shows graphs of the field distribution at the channel axis vs. the radius R. As can be seen, the field in the channel first changes slowly and then drops rapidly, forming a steep barrier, as it were. This property of the field in

selecting electrode. As V_a increases, the plasma will be ejected back into the emission channel. In this event there will be an increase in the boundary density and the temperature of the plasma and, on the basis of (7), the boundary gradient will increase. A further increase in V_a results in a shift of the plasma boundary into the inner cavity of the emission channel. Here, because of a strong longitudinal magnetic field and increased pressure

STOP HERE

STOP HERE

FIRST LINE OF TEXT

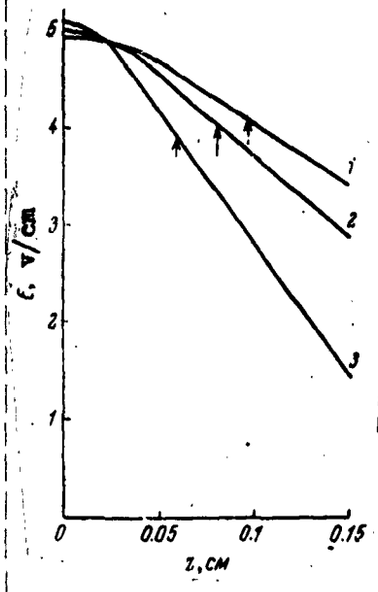

Fig. 4. Graphs of the distribution of an electric field on the channel axis. 1) R = 0.04 cm; 2) R = = 0.06 cm; 3) R = 0.08 cm; z is the axial coordinate. The arrows indicate possible plasma boundaries at V_a = 60 kv.

NE OF TITLE

the channel is very convenient for selecting ions, since it makes it possible for the plasma to approach the region of the strong electric field which, on the strength of (1), should result in increased ion-current density.

Let us give certain estimates. From (8) we can show that the depth of penetration d of a certain equipotential of the undisturbed external field with $v = v_d$ into the channel is proportional to R. On the other hand, it has been experimentally verified that the value of the undisturbed potential at the axis of the channel input v_0 is also proportional to R. We will consider that the undisturbed potential v_0 changes little on passage of an ion current when the plasma boundary is within the channel. This assumption was based on the following facts: 1) since there is a strong magnetic field in the emission channel, the conditions for current flow will be analogous to the case of infinite electrodes, i.e., $\alpha = 1$; 2) there is no magnetic field in region II (Fig. 3), and therefore $\alpha > 1$, resulting in a decrease in the potential drop along the beam.

Then, because of (2) and our assumptions, we can write

$$I = \frac{5.45 \cdot 10^{-8}}{\sqrt{A}} \frac{v_0^{5/2} S\beta(R)}{d^2} \sim \beta v_0^{5/2} \sim \beta R^{5/2}, \qquad (10)$$

$$j \sim \frac{\beta(R)}{R^{1/2}}, \qquad (11)$$

where $\beta(R)$ is a function that takes into account the distribution of plasma density through the pinch cross section.

Let us estimate the dependence of the utilization factor of the working gas Y on the channel radius. Since in the case of a low degree of plasma ionization (in ion sources the degree of ionization does not exceed several per cents) the gas flow through a short capillary is not extensive,

STOP HERE STOP HERE

FIRST LINE OF TEXT

$$\gamma = \frac{I}{Q} \sim \frac{\beta(R)}{R^{1/2}}. \qquad (12)$$

From (10), (11), and (12) it is evident that with increasing channel radius the ion current should increase as $R^{3/2}$, if $\beta(R)$ is increased correspondingly, while the current density and the useability of the gas should decrease as $R^{-1/2}$.

4. The Experiment

We have given a detailed description of the experimental apparatus in a previous paper [10]. FIRST LINE OF TITLE We used, as our ion source, the Ardenne duoplasmatron [11] with changes in the region of ion selection. The anode of the source was a copper disc 3 mm thick, cooled with running water. The experiments were conducted for R = = 0.04, 0.055, 0.06, and 0.08 cm. The ion source, focused by a unipotential electrostatic lens, was measured on the receiver (a Faraday cylinder) by the calorimetric method [12]. The selection of the ion current on the electrodes of the ion optic was measured [13], and at $V_a > 25$ kv was negligible.

Figure 5 shows the ion current at the receiver, I_r, vs. R when $V_a = 60$ kv and for an arc-source of current $I_a = 1.4$ amp (curve 1). Curve 2 was constructed in relative units without consideration of β (uniform cross-sectional density); as the base we used the point for which R = 0.04 cm. It can be seen that curves 1 and 2 diverge sharply with increasing R. The average plasma density vs. emission-channel radius (the function $\beta(R)$) was determined experimentally [10], and is shown in Fig. 5 by curve 4. Curve 3 was constructed on the basis of curve 2, taking into account $\beta(R)$. It can be seen that the experimental and calculated curves are in quite good agreement.

It was to be expected that as the current of the duoplasmatron arc increased, in addition to an increase in $\beta(R)$ there would be a corresponding increase in the output ion current; however, attempts to prove this gave negative results. For working with focused arc currents it is necessary to increase the pressure of the

STOP HERE STOP HERE

working gas in the duoplasmatron; this resulted in increased gas pressure in the ion-selection gap, due to which an arc discharge is ignited between the selecting electrode and and anode of the source. Because of this, the maximum arc current in our experiments was 1.4 amps.

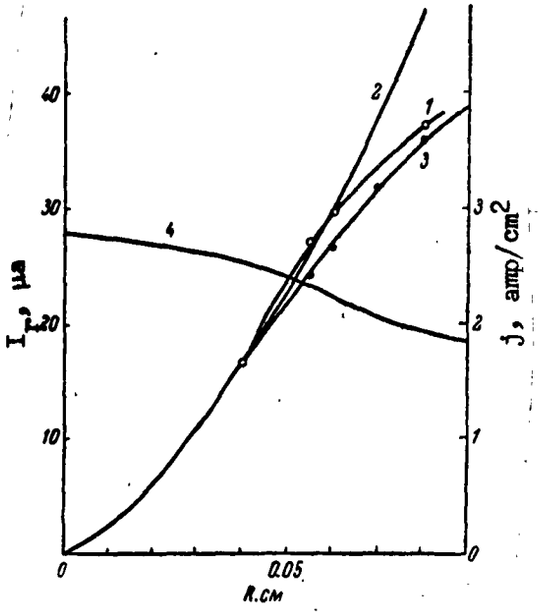

Fig. 5. Selected ion current I vs. R for V_a = 60 kv. 1) experimental curve; 2) dependence calculated from the 3/2 law; 3) the same, taking into account β(R); 4) distribution of ion-current density at the plasma boundary j = β(R).

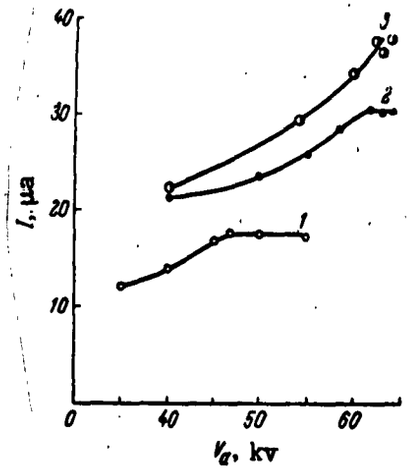

Fig. 6. Output ion current T vs. selection potential V_a. 1) R = 0.04 cm; 2) R = 0.06 cm; 3) R = 0.08 cm.

Figure 6 shows I_r vs. V_a for various R. As can be seen, the dependences first increase, and then saturation sets in due to the finite emissivity of the plasma for the given arc current I_a. From the value of the saturation currents, on the basis of (2), we can determine the location of the plasma boundary at the start of emission. The value of v_o was determined using an electrolytic bath, and was 3.6, 4.5, and 5.1 kv for openings R = 0.04, 0.06, and 0.08, respectively, with V_a = 60 kv. On this basis, d = 0.06, 0.08, and 0.10 cm, respectively. Since the thickness of the anode was 0.3 cm, the plasma-emission boundary, as can be seen, was within the emission channel. Thus we can use the emission-channel cross-sectional area as the plasma-emission surface.

FIRST LINE OF TEXT

Let us calculate the plasma density n_o in the emission channel. The ion current in the emission channel is defined as $I_r = n_o v_i e S$, where I_r is the measured ion current at the receiver; v_i is the mean directional velocity of the plasma ions; e is the electron charge; and S is the emission channel cross section. Then,

$$n_0 = 4.5 \cdot 10^{12} \frac{I_r}{\sqrt{v_i} S},$$

I_r is in amperes; $v_i \approx 1$ ev [14]; n_o is $1/cm^3$; and S is in cm^2.

From the curves in Fig. 6 we get $n_o = 0.65$ to $1.2 \cdot 10^{13}$. Bohm's formula [7] gave approximately the same results.

FIRST LINE OF TITLE

Taking $n_o = 10^{13}$ and $T_e = 10^5$ °K, on the basis of (7) we find that the potential gradient at the plasma boundary should be ≈ 20 kv/cm.

In Fig. 4 the arrows indicate the position of the plasma boundary according to calculations. As can be seen, the boundaries are positioned for a value of ≈ 10 kv for the undisturbed potential. A disturbance of the external field results in a change in the potential gradient to a value defined by (7).

Conclusions

On the basis of the foregoing we can draw the following conclusions:

1. The ion current selected from a plasma source is limited by the space charge.

2. The maximum ion-current density per emission-channel cross section is attained for those values of a when the plasma-emission boundary is within the emission channel.

3. Knowing the distribution of the average plasma density in the emission channel, and the electron temperature, we can calculate approximately, on the basis of (7), (10), (11), and (12), for given R, the value of the selection current I_r, the current density in the emission channel j, and the useability of the working gas Y.

STOP HERE

STOP HERE

I would like to thank V. I. Krasnovskiy for participating in all the experiments, B. K. Shembel' and I. I. Slivkov for their support and helpful advice, and D. V. Karetnikov and N. V. Pleshivtsev for their help in the work.

References

1. J. Langmuir. Phys. Rev., 2, 450, 1912.
2. I. I. Levitov. Doklady AN SSSR, 84, 1247, 1952.
3. J. Kistemaker and D. Dekker. Physica, 16, 198, 1950.
4. J. Kistemaker. Physica, 16, 209, 1950.
5. M. D. Gabovich and Ye. T. Kucherenko. Zhurnal Tekhnicheskoy Fiziki, 26, 996, 1956.
6. ibid., 27, 299, 1957.
7. D. Bohm. The Characteristics of Electrical Discharges in Magnetic Fields. New York, 1949.
8. P. C. Thoneman and E. R. Harrison. AERE, GP/R, Harwell, 1958.
9. F. Gray. The Bell System Technical Journal, 18, 1, 1939.
10. S. N. Popov. Pribory i Tekhnika Eksperimenta [PTE], No. 4, 20, 1961.
11. M. Ardenne. Tabellen der Elektronenphysik. Berlin, 1956.
12. V. A. Yegorov, D. V. Karetnikov, and S. N. Popov. PTE, No. 2, 1960.
13. S. N. Popov. PTE, No. 4, 69, 1961.

Institute of Chemical Physics
Academy of Sciences of the USSR
Moscow

Submitted
October 17, 1960.

DISTRIBUTION LIST

DEPARTMENT OF DEFENSE	Nr. Copies
HEADQUARTERS USAF	
AFCIN-3D2	1
OTHER AGENCIES	
CIA	1
NSA	2
AID	2
OTS	2
AEC	2
PWS	1
PGE	1
RAND	1

MAJOR AIR COMMANDS	Nr. Copies
AFSC	
SCFTR	1
ARO	1
ASTIA	10
TD-Bla	3
RADC (RAY)	1
SSD (SSF)	1
ASD (DCF)	1
ESD (ESY)	1
AFMTC (MTW)	1
APGC (PGF)	1
AFSWC (SWY)	1
AFFTC (FTY)	1